Residential buildings with heat pumps, a verified bottom-up model for demand side management studies

Dieter Patteeuw[1], Lieve Helsen[1,*]

[(1)] Applied Mechanics and Energy Conversion, Department of Mechanical Engineering, KU Leuven, Belgium, Email: lieve.helsen@kuleuven.be

1. ABSTRACT

The increasing use of intermittent renewable energy sources has reawakened the interest for demand side management, among which thermostatically controlled loads are a much mentioned option. One of these load types are residential buildings equipped with heat pumps, which can shift electricity consumption in time without compromising indoor thermal comfort. A prerequisite for the widespread application of this technology is a thorough understanding of its potential for demand side management. This type of studies needs models which on the one hand are computationally efficient enough to be scaled up to a country's building stock but on the other hand are still a correct system representation. These issues are tackled by considering multiple levels of detail in reduced order models and verifying these models to a detailed simulation model. A second step is the aggregation of buildings with different occupant behavior. The aggregation's performance is assessed by comparing the response to various electricity price profiles. Results show that the proposed aggregated model is sufficiently accurate in representating the considered buildings. The methodology presented in this paper can also be applied to other building types, resulting in an aggregated and verified model of a country's building stock for demand side management studies.

Keywords: residential building, heat pump, demand side management, linear model, reduced order model, aggregated model

2. INTRODUCTION

Demand side management (DSM) is the altering of consumer's electricity demand in order to obtain a more desirable load shape for utilities (Gellings, 1985). Strbac (2008) states that such shifting of electricity demand can have numerous benefits such as reducing the need for back-up power plants, grid investments and so on. He identified two main drivers for an increasing potential of DSM, being the increase in renewable energy sources and the improvement of information and communication technologies. Heat pumps are often regarded as a promising technology for DSM, for example to increase voltage security (Wang et al., 2012) or to increase the usage of wind energy (Hedegaard, Mathiesen, Lund, & Heiselberg, 2012). One of the factors hampering its widespread application is a lack of understanding of the potential benefits (Strbac, 2008) which requires appropriate models to enable estimating the potential. This paper aims at presenting a model which can be used to study the flexibility potential of residential buildings equipped with heat pumps. This can be done by means of co-optimization of the presented model and state of the art electricity generation park models. Bruninx, Patteeuw, Delarue, Helsen, and D'haeseleer (2013) showed the added value of this co-optimization, as it can be used to assess the potential of applying DSM. The electricity generation park model is a mixed integer linear optimization problem, which sets requirements for the building and heating system model structure (see section 3.2.1 and section 3.2.2).

Studies on the DSM potential of buildings equipped with heat pumps tend to focus on either the buildings energy demand or on the electricity generation park. The former studies focus on one

building or a limited cluster of buildings, using existing building performance simulation tools (e.g. Kelly, Tuohy, and Hawkes (2013); Henze, Felsmann, and Knabe (2004)) or experiments (e.g. Kok et al. (2012)). The disadvantage of these studies is that the electricity generation system is simplified to a fixed electricity price profile, sometimes leading to spectacular cost savings, going up to 57% (Henze et al., 2004). This potential benefit might diminish when the market penetration of these flexible systems increases (Bruninx et al., 2013).

An increasing number of DSM potential studies models both electricity generation park and buildings simultaneously. Typically, these studies start from an electricity generation park model (Eq. (1)-(3)) in which the operational cost $cost_{op}$ of generating electricity gen_j is minimized over a certain time period, with j being the time step. The flexibility in electricity demand offered by the buildings with heat pumps, is modelled as follows. The heat pumps cause an additional electricity demand $P_j^{hp,tot}$ which is limited by a linear state space model (Eq. (4)) of building and hot water tank temperatures T_j , comfort constraints (Eq. (5)) and power constraints (Eq. (6)). The overall model is hence the following optimization problem:

$$\underset{gen_j, P_j^{hp,tot}, T_j}{\text{minimize}} \quad \sum_j cost_{op}(gen_j) \tag{1}$$

$$\text{subject to} \quad \forall j : con_{op}(gen_j) = 0 \tag{2}$$

$$\forall j : gen_j = demand_j + P_j^{hp,tot} \tag{3}$$

$$\forall j : P_j^{hp,tot} = ss(T_j) \tag{4}$$

$$\forall j : comfort(T_j) \geq 0 \tag{5}$$

$$\forall j : power(P_j^{hp,tot}) \geq 0 \tag{6}$$

in which equation (3) makes sure that at each time step, the total electricity generation gen_j covers the traditional electricity demand $demand_j$ and the additional electricity demand $P_j^{hp,tot}$. These studies tend to oversimplify the building: a heat pump is often considered to have a constant coefficient of performance (COP) while solar heat gains and thermal energy storage in the building structure are often neglected. Regarding the COP, only two studies could be found that have a more complicated representation of the COP, namely by considering the COP either linearly (Good, Navarro-espinosa, Mancarella, & Karangelos, 2013) or non-linearly (Wang et al., 2012) dependent on ambient air temperature. Solar heat gains are sometimes indirectly included by considering these as part of the model's white noise (Callaway, 2009; Kamgarpour et al., 2013). In order to shift a heat pump's electricity demand in time without compromising the users' comfort, some thermal energy storage must be present in the system. This can be either in storage tanks (active thermal storage) or in the building structure itself (passive thermal storage). Some authors focussing on active thermal energy storage in domestic hot water tanks (Barton et al., 2013; Kondoh, Lu, Member, & Hammerstrom, 2011) or high capacity space heating systems (Long, Xu, & He, 2011; Meibom et al., 2007) consider buildings as providers of a fixed thermal energy demand profile, hereby neglecting the energy storage potential of the building structure.

In order to determine the DSM potential of passive energy storage, the building structure is in some cases represented by two (Pedersen, Andersen, Nielsen, Stæ rmose, & Pedersen, 2011; Wang et al., 2012) or three thermal capacities (Hedegaard & Balyk, 2013). In general though, only one thermal capacity is considered (Good et al., 2013; Hedegaard et al., 2012; Muratori, Roberts, Sioshansi, Marano, & Rizzoni, 2013). Modelling the building structure as one thermal capacity allows statistical aggregation techniques in order to study the DSM potential of large

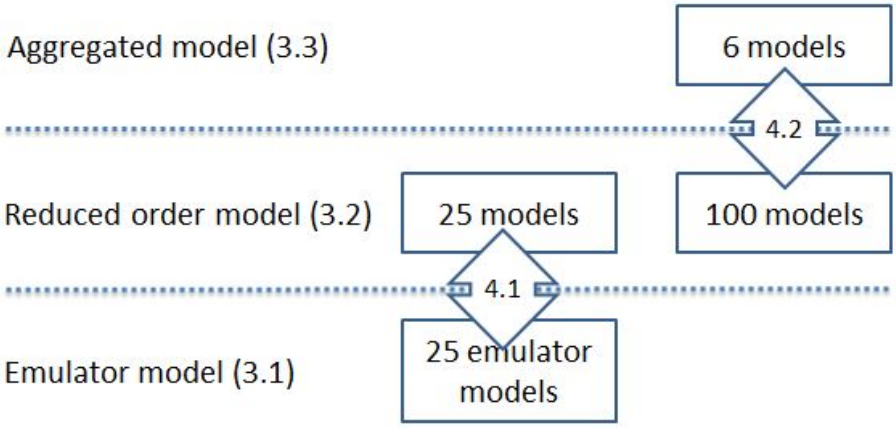

Figure 1: The aim of the paper is to develop an aggregated model which is derived from a detailed building simulation (emulator) model. Section 4.1 compares multiple reduced order models to this emulator model. In section 4.2 the aggregated model is compared to a large set of these reduced order models.

sets of buildings (Malhame, 1985; Kamgarpour et al., 2013; Callaway, 2009). Another advantage is that the model becomes similar to that of other thermostatically controlled loads, such as fridges and freezers, allowing similar modelling techniques (Lu & Vanouni, 2013; Mathieu, Dyson, & Callaway, 2012). One could argue which level of detail is needed to describe the transient behaviour of a building. This is discussed in section 3.2.1.

The aim of this paper is to present a set of equations in the form of Eq. (4)-(6) that accurately represents the DSM potential of thousands of buildings equipped with heat pumps. In order to achieve feasible computation times, an aggregated, reduced order model of these buildings is required. This paper presents three levels of modelling detail and a procedure to verify the top-level aggregated, reduced order model (see figure 1). The highest level of detail can be found in the building performance simulation model, which acts as the emulator model. From this, a reduced order model (ROM) is deducted. A second level of simplification aggregates multiple of these ROMs, based on their occupants behaviour. The results section shows the comparison between the different levels of details, linking the performance of the most detailed model to the top-level aggregated ROM model. The discussion section elaborates on this comparison, to support the conclusions in the conclusion section.

3. METHODOLOGY

This section describes three levels of modelling detail (Figure 1). The first model (section 3.1) is a fully physical model which acts as an emulator model. From this, multiple reduced order models are deduced (section 3.2). The final level of simplification is the aggregation of multiple buildings by a mathematical operation on the comfort bounds (section 3.3).

3.1. Emulator model

A detailed emulator model of the building is developed using the IDEAS library in Modelica, described by Baetens et al. (2012). This modelling environment has been verified and validated using the BESTEST methodology (Judkoff & Neymark, 1995). The parameters for the single zone building are taken from Reynders, Diriken, and Saelens (2014), who interpreted the parameters of a typical post 2005 built Belgian dwelling as described in the TABULA project (Cyx, Renders, Van Holm, & Verbeke, 2011). The building has a floor surface of 270 m^2 and

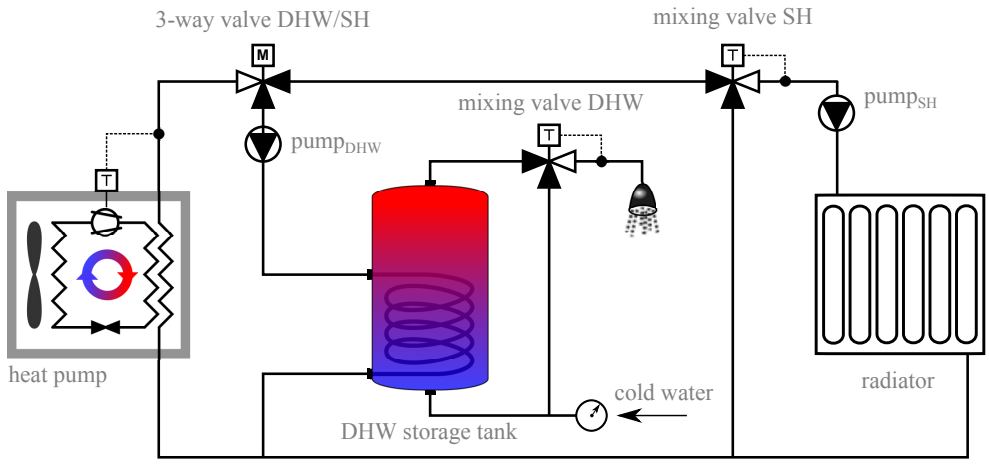

Figure 2: Hydraulic scheme of the heating system, based on De Coninck et al. (2014). A modulating air coupled heat pump supplies heat for domestic hot water (DHW) via a storage tank and space heating (SH) via a radiator.

a protected volume of $741\ m^3$. The combination of infiltration and ventilation cause 1.5 air changes per hour. The exterior walls, roof and windows have a U-value of $0.4\ \frac{W}{m^2K}$, $0.5\ \frac{W}{m^2K}$ and $1.4\ \frac{W}{m^2K}$ respectively. In each cardinal direction, the building has an average of about $10\ m^2$ window surface, resulting in a percentage glazing of 22%. The Belgian climate is considered, based on the measurements in Uccle and distributed by Meteonorm (*METEONORM Version 6.1 Edition 2009*, 2009).

The heating system is also modelled using the IDEAS library. It consists of a modulating air coupled heat pump supplying both warm water to a radiator for space heating (SH) and a domestic hot water (DHW) tank(Figure 2). All components are based on physical equations, while the parameters for these components are determined from either manufacturer data or empirical correlations. A full description of the heat pump model, along with a validation of the domestic hot water tank model is described by De Coninck, Baetens, Saelens, Woyte, and Helsen (2014). The model for the radiator is described by Baetens et al. (2012). The heat pump and radiator are sized to meet 80% of the design heat demand of $8900W$, in accordance with the code of good practice in Belgium ("Code van goede praktijk voor de toepassing van warmtepompsystemen in de woningbouw", 2004).

Table 1: Multiple buildings are considered having a different number of occupants with each their own DHW tank for supplying domestic hot water.

Household size [Persons]	1	2	3	4	5	6
Number of households (25 case)	8	8	4	3	1	1
Number of households (100 case)	32	32	16	12	4	4
Daily DHW demand at $50\,°C$ [liter]	62.5	125	162	200	237	300
DHW tank size [liter]	120	160	160	200	300	300
DHW tank UA [W/K]	0.117	0.098	0.098	0.085	0.085	0.077

Since the model is aimed to be scaled up in order to represent thousands of buildings, also various numbers of occupants per house are considered. To this aim, 25 buildings are considered, each having the same building structure, but with different number of occupants and different occupant behaviour (Table 1). For the aggregation method, the aggregated model was compared to 100 ROMs, each having again the same building model but different occupant behaviour. The

household size determines the daily DHW demand, which is based on Peuser, Remmers, and Schnauss (2010). This daily demand determines the size of the DHW tank. The parameters of the tanks are based on the Vitocell 100-W gamma of Viessmann.

3.2. Reduced order model

The reduced order model describes the dynamic behaviour of both building and heating system with fewer equations and detail than the emulator model. This ROM is the set of linear equations (4)-(6) that still describes the flexibility in electricity use provided by the presented system. In order to obtain profiles of how the ROM performs with respect to the emulator model (figure 5), the optimization problem (Eq. (1)-(6)) is reduced to:

$$\underset{P_j^{hp,tot},T_j}{\text{minimize}} \quad \sum_j cost_j \cdot P_j^{hp,tot} \tag{7}$$

$$\text{subject to} \quad \forall j : P_j^{hp,tot} = ss(T_j) \tag{8}$$

$$\forall j : comfort(T_j) \geq 0 \tag{9}$$

$$\forall j : power(P_j^{hp,tot}) \geq 0 \tag{10}$$

in which $cost_j$ is the electricity cost at time step j (Figure 8(a)). Thus given a specific electricity price profile, the optimization gives a resulting electricity consumption and temperatures, which can be compared to the emulator model.

A linear model of the building was already developed by Reynders et al. (2014) and is described shortly in section 3.2.1. This paper mainly focuses on the reduced order model of the heating system. Table 2 summarizes various aspects of the heating systems that can be modelled in different ways. Section 3.2.2 describes in detail the multiple representations for the heat pump. Section 3.2.3 focuses on the DHW tank and finally section 3.2.4 describes the radiator model.

Table 2: Component model description for the emulator model. Per component two options for the reduced order model (ROM) are considered. T_{amb} is the ambient air temperature. P^{hp} is the electrical power used by the heat pump.

Component	Emulator model	ROM option 1	ROM option 2
Heat pump COP	Interpolation of manufacturer data	Constant COP, average from correlation	COP from correlation, function of T_{amb}
Heat pump modulation	Interpolation of manufacturer data	mixed integer formulation (Eq.12-15)	linear in P^{hp} (Eq.16-19) + post processing
DHW storage tank	multiple layers with energy balance equation	fully mixed with mixed integer constraint (Eq.22-23)	fully mixed with linear constraint (Eq.24-29)
Radiator	radiator formula and one thermal capacity	no radiator model	linearised heat transfer and one thermal capacity (Eq.30)

3.2.1. Building model

Reynders et al. (2014) deducted a linear model with five states (Figure 3(a)) by performing system identification on the emulator model described in section 3.1. These five states are the indoor operative temperature T_{air} and the temperature of inner walls T_{wi}, roof T_{roof}, floor T_f and

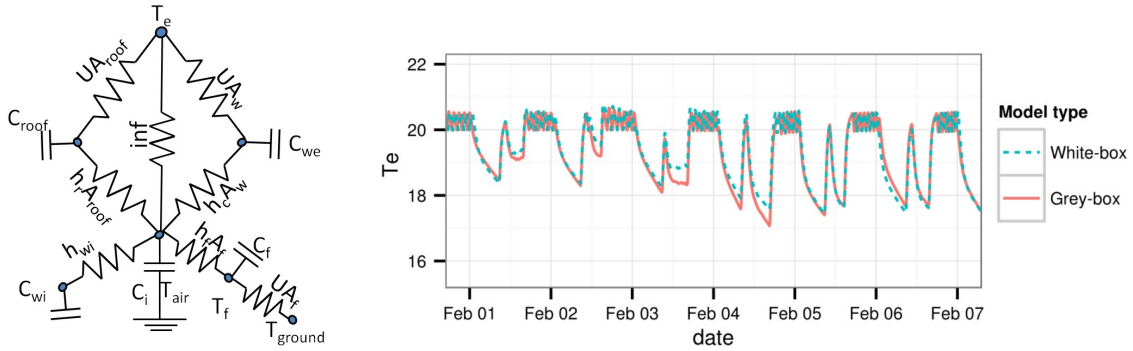

(a) Linear building model.

(b) Comparison of indoor temperature for linear (Grey-box) and detailed physical (White-box) model

Figure 3: The linear model (left) comprises of five thermal capacities and hence five states. It is a model able to approximate the behaviour of the detailed physical model (right). Source: Reynders et al. (2014).

exterior walls T_{we}. The thermal capacities and heat transfer coefficients associated with these states have the same indices. Inputs to the model are the ambient air temperature T_e, ground temperature T_{ground} and the heat gains due to solar irradiation, internal gains and radiators. Multiple linear models were considered, from which the five states model clearly outperforms the rest. This model shows an RMSE error of only $0.3\,°C$ on a two day ahead prediction of the indoor operative temperature of the detailed physical model. Figure 3(b) shows the comparison between both models. The linear model can be written in the following state space structure for a certain time step j:

$$\dot{T}_j = A \cdot T_j + B \cdot U_j \tag{11}$$

in which T_j and U_j are vectors with the above mentioned states and inputs respectively. The parameters in the matrices A and B were determined from system identification. This five states model is used as part of the ROM in this paper.

3.2.2. Heat pump model

This paper focuses on modulating heat pumps for which the performance strongly depend on the supply and source temperature, and on the modulation. Verhelst, Logist, Van Impe, and Helsen (2012) studied multiple representations of the heat pump COP based on these variables, among which non-linear representations. Since the ROMs discussed in this paper are intended to be combined with electricity generation park models (Bruninx et al., 2013), a non-linear representation is out of the question, hence only linear and mixed integer representations of heat pump performance are allowed. The two remaining options for this framework are thus a constant COP or a COP that is a function of the ambient air temperature only. The heat pump integrated in the emulator model can supply warm water to both space heating (SH) and domestic hot water (DHW), hence the decision variables are the electric power of the heat pump to supply space heating $P_j^{hp,sh}$ or domestic hot water $P_j^{hp,dhw}$ at time step j. The most detailed mixed integer representation of the heat pumps performance is the set of equations (12)-(15).

The equations for the domestic hot water supply are analogous to (12)-(14).

$$\forall j : P_j^{hp,sh} = P_j^{min,hp,sh} \cdot z_j^{hp,sh} + P_j^{int,hp,sh} \tag{12}$$

$$\forall j : 0 \leq P_j^{int,hp,sh} \leq (P_j^{max,hp,sh} - P_j^{min,hp,sh}) \cdot z_j^{hp,sh} \tag{13}$$

$$\forall j : \dot{Q}_j^{hp,sh} = COP_j^{i,sh} \cdot P_j^{min,hp,sh} \cdot z_j^{hp,sh} + P_j^{int,hp,sh} \cdot (COP_j^{a,sh} - COP_j^{i,sh}) \tag{14}$$

$$\forall j : z_j^{hp,sh} + z_j^{hp,dhw} \leq 1 \tag{15}$$

This representation has the advantage of being directly convertible to control signals for the heat pump and the pumps connecting the heat pump to the DHW tank and space heating by means of the integer variables $z_j^{hp,dhw}$ and $z_j^{hp,sh}$ that can only be zero or one. It is also possible to take into account a different COP at full load $COP_j^{a,sh}$ and at minimal modulation $COP_j^{i,sh}$. The power that the heat pump consumes does not violate the working constraints, it is either off or between the maximal $P_j^{max,hp,sh}$ and minimal $P_j^{min,hp,sh}$ modulating power. The integer power level $P_j^{int,hp,sh}$ is a dummy variable to cope with these constraints. The disadvantage is the number of integers used, since these are known to cause the calculation time to explode. Solvers for mixed integer linear problems can typically handle problems with up to 10^5 integers, however when exceeding this order of magnitude, this becomes a lot harder (Koch et al., 2011). Considering a time horizon of 48 hours with two integers each hour per house, this would limit the number of buildings in one optimization problem to 104 buildings.

Another option to represent the heat pump is a linear model (16)-(19), in which the electric power of the heat pump towards space heating or domestic hot water can vary between 0 and $P_j^{max,hp}$, as long as the sum of the two remains below $P_j^{max,hp}$. Linear optimization models are computationally very efficient to solve, the optimization takes only some seconds on a regular laptop while the mixed integer representation (12)-(15) can easily take minutes to hours to solve. This linear model consists of the following equations:

$$\forall j : P_j^{hp,sh} + P_j^{hp,dhw} \leq P_j^{max,hp} \tag{16}$$

$$\forall j : P_j^{hp,sh}, P_j^{hp,dhw} \geq 0 \tag{17}$$

$$\forall j : \dot{Q}_j^{hp,sh} = COP_j^{sh} \cdot P_j^{hp,sh} \tag{18}$$

$$\forall j : \dot{Q}_j^{hp,dhw} = COP_j^{dhw} \cdot P_j^{hp,dhw} \tag{19}$$

The disadvantage of the linear optimization model is the extra effort needed to derive control signals for the individual heat pump and circulation pumps, respecting the lower modulation level of the heat pump. To this aim, a post processing is applied in order to obtain feasible profiles for 'scheduled operation' as explained by Kosek, Costanzo, Bindner, and Gehrke (2013). Since multiple buildings are controlled at once, the electricity demand per building can be redivided among the buildings, as long as the sum of these electricity demands remains the same. In this way, some buildings that require less than the minimal modulation of the heat pump, are switched off and this difference is made up for in other buildings. The buildings from which the heat pumps were switched off, are compensated for this fact in a later time step.

3.2.3. Domestic hot water tank

The central component in the DHW model is the DHW tank. This tank can either be modelled as perfectly stirred or perfectly stratified. The latter storage tank model was not considered in this study, since it was noticed in the simulations of the emulator model, that the heat exchanger usually destroys the thermal stratification. The tank is thus assumed to be a perfectly stirred

water tank, meaning that all water in the tank is at the same temperature T_j^{tank} at time step j. The water in the DHW tank can either be heated up by the heat pump, $\dot{Q}_j^{hp,dhw}$ or by a back up electrical heater $\dot{Q}_j^{aux1,dhw}$. Heat is extracted from the DHW tank through demand for hot water $\dot{Q}_j^{dem}$ and heat loss to the surroundings. The discretized version of the energy balance for the DHW tank leads to the following equation:

$$\forall j: \quad \rho c_p V_{tank} \frac{T_{j+1}^{tank} - T_j^{tank}}{\Delta t} = \dot{Q}_j^{hp,dhw} + \dot{Q}_j^{aux,dhw} - \dot{Q}_j^{dem} - UA \cdot (T_j^{tank} - T_j^{surr}) \quad (20)$$

with $\rho[kg/m^3]$ and $c_p[J/kgK]$ the density and heat capacity of water and $V_{tank}[m^3]$ the volume of the tank. With Δt the time step of the optimization, the time derivative of T_j^{tank} is approximated as $\frac{T_{j+1}^{tank} - T_j^{tank}}{\Delta t}$. The term $UA \cdot (T_j^{tank} - T_j^{surr})$ determines the heat loss to the surroundings, which is at temperature T_j^{surr}. The thermal conductance $UA[W/K]$ is that of the insulation around the DHW tank, which is the dominant resistance to heat transfer.

The temperature of the cold tap water T^{cold} and the temperature of the supplied DHW T^{dem} are both assumed to be constant. A lower boundary for the temperature of the water in the DHW tank stems from the demand for a comfortable temperature of DHW. Since the tank is perfectly stirred, the whole tank must be heated up to at least T^{dem} when the occupants desire hot water. In the meantime, the water in the tank can get as low as T^{cold}:

$$\forall j: \quad T_j^{tank} \geq T^{dem} \cdot hwd_j + T^{cold} \cdot (1 - hdw_j) \quad (21)$$

with $hwd_{\mathrm{s,j}}$ a binary parameter which is 1 when hot water is demanded in time step j and 0 when this is not the case. The water in the DHW tank can be at a higher temperature than what is demanded, in which case a three way valve is used to mix it with the cold water to the desired temperature. Given the constant T^{cold} and T^{dem} and the fact that the whole tank is above T^{dem} in case of DHW demand, $\dot{Q}_j^{dem}$ is independent of the tank temperature (Patteeuw, Bruninx, Delarue, D'haeseleer, & Helsen, 2013).

The heat pump can deliver heat up to a maximum temperature T_{max}^{hp}, typically $60\,^{\circ}C$, which is lower than the maximum allowed temperature of the DHW tank T_{max}^{tank}, typically $90\,^{\circ}C$. This difference introduces the need for a boolean variable z_j^{dhw} and the following constraints

$$\forall j: \quad T_j^{tank} + \frac{\Delta t}{\rho \cdot V_{tank} \cdot c_p} \cdot \dot{Q}_j^{hp,dhw} \leq (1 - z_j^{hwd}) \cdot T_{max}^{hp} + z_j^{hwd} \cdot T_{max}^{tank} \quad (22)$$

$$\forall j: \quad \frac{\dot{Q}_j^{hp,dhw}}{COP_j^{hp,dhw}} \leq (1 - z_j^{hwd}) \cdot P_{max}^{hp} \quad (23)$$

When z_j^{hwd} is zero, the temperature of the DHW tank is lower than T_{max}^{hp} and the heat pump's output is limited by either the temperature up to which it can heat, Eq. (22), or by its maximal electrical power, Eq. (23). In case z_j^{hwd} is one, the temperature of the DHW tank is higher than T_{max}^{hp} and the heat pump's output is zero through Eq. (23). In that case, Eq. (22) becomes an upper constraint on the temperature of the DHW tank.

The boolean z_j^{hwd} makes the problem a mixed integer linear problem, with the above mentioned problems. A linear alternative for the model is defining the tank temperature T_j^{tank} as the sum of a temperature which is influenced by the heat pump T_j^{hp} and a temperature difference influenced by the auxiliary heater dT_j^{aux} (the latter for the temperature range above $60\,^{\circ}C$). The model

hence becomes:

$$\forall j: \quad \rho c_p V_{tank} \frac{T_{j+1}^{hp} - T_j^{hp}}{\Delta t} = \dot{Q}_j^{hp,dhw} + \dot{Q}_j^{aux1,dhw} - \dot{Q}_j^{hp,dem} - UA \cdot (T_j^{hp} - T_j^{surr}) \quad (24)$$

$$\forall j: \quad \rho c_p V_{tank} \frac{dT_{j+1}^{aux} - dT_j^{aux}}{\Delta t} = \dot{Q}_j^{aux2,dhw} - \dot{Q}_j^{aux,dem} - UA \cdot (dT_j^{aux}) \quad (25)$$

$$\forall j: \quad \dot{Q}_j^{hp,dem} + \dot{Q}_j^{aux,dem} = \dot{Q}_j^{dem} \quad (26)$$

$$\forall j: \quad \dot{Q}_j^{aux1,dhw} + \dot{Q}_j^{aux2,dhw} = \dot{Q}_j^{aux,dhw} \quad (27)$$

$$\forall j: \quad T_{max}^{hp} \geq T_j^{hp} \geq T^{dem} \cdot hwd_j + T^{cold} \cdot (1 - hdw_j) \quad (28)$$

$$\forall j: \quad (T_{max}^{tank} - T_{max}^{hp}) \geq dT_j^{aux} \geq 0 \quad (29)$$

The heat demand $\dot{Q}_j^{dem}$ for supplying DHW has to be extracted either from the heat pump influenced temperature $\dot{Q}_j^{hp,dem}$ or from the auxiliary influenced temperature $\dot{Q}_j^{aux,dem}$. The heat pump can hence only heat up T_j^{hp} to T_{max}^{hp}. The auxiliary heater can supply heat to both the heat pump influenced temperature ($\dot{Q}_j^{aux1,dhw}$) and the auxiliary heater influenced temperature ($\dot{Q}_j^{aux2,dhw}$).

3.2.4. Heat emission system

The heat emission system is a radiator, that is modelled as a thermal capacity C_{rad} at a temperature T_j^{rad}:

$$\forall j: \quad C_{rad} \frac{T_{j+1}^{rad} - T_j^{rad}}{\Delta t} = \dot{Q}_j^{hp,sh} + \dot{Q}_j^{aux,sh} - (UA)_{rad} \cdot (T_j^{rad} - T_j^{zone}). \quad (30)$$

The thermal capacity of the radiator $C_{p,rad}$ is the sum of the thermal capacities of the radiator's dry mass and water content. The constant overall heat transfer coefficient $(UA)_{rad}$ is attained by linearising the radiator formula around the design supply temperature.

3.3. Aggregated model

In order for a building model to represent thousands of buildings, the same building model is considered multiple times, each time with a different user behaviour. The motivation to model multiple buildings with different user behaviour, is to attain a reasonable load diversity in order to avoid an unrealistically high peak load. In the field of electricity distribution systems, Kersting (2012) concluded that considering the electricity demand of 70 buildings is enough to represent the load diversity of a much larger cluster of buildings. In this paper, some margin was taken and 100 buildings were considered. The number of inhabitants in each building was chosen in such a way that it represents the population structure in Belgium (FOD economy Belgium, 2008), see Table 1.

The methodology presented in this section can be applied for any occupancy schedule. For this study in particular, time profiles of how many occupants are present and awake in the building were extracted from the model of Richardson, Thomson, and Infield (2008). This data is processed in order to get the thermal comfort limits for the building: if at least one occupant is present and awake during at least half an hour, the lower temperature set-point becomes $20\,°C$ instead of $16\,°C$. Based on Peeters, Dear, Hensen, and D'haeseleer (2009), an upper bound for the indoor operative temperature is on average $24\,°C$. The hot water demand at $60\,°C$ is inspired by Peuser et al. (2010), namely 50 litre per person for the first two inhabitants and

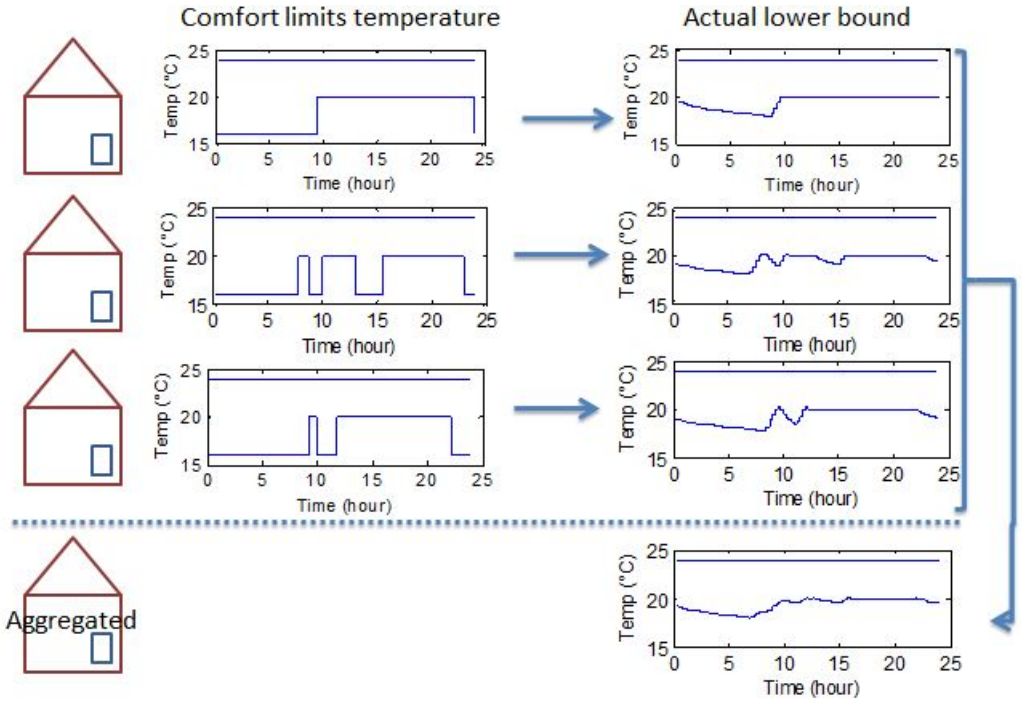

Figure 4: Concept of the aggregation. For multiple buildings with identical building structure but different user behaviour, the actual lower temperature limits are determined from the occupant's temperature set-points. The aggregated model then has the same building structure, but a lower bound for the indoor operative temperature which is the mean of the actual lower temperature limits of the larger cluster of buildings.

30 litre per person for the following number of inhabitants. For each number of inhabitants, one or two tap moments are generated during the periods the occupants are present. These tap moments are distributed in such a way that the sum of the hot water demand for all 100 buildings corresponds to the profile denoted by Peuser et al. (2010). This aggregated hot water tapping profile was measured from a very large apartment building in Germany.

A cluster of hundred building models, even if all these models are linear, is still a large problem to solve. A method is thus needed to reduce the number of buildings, namely by aggregation. In this paper, a new methodology is presented to aggregate building models which have the same physical parameters but different user behaviour. This methodology is illustrated in figure 4. Assume that the 32 households consisting of one person from Table 1 have the same building structure and the same hot water storage tank. Most of the models for these 32 households will be similar, except for the fact that these will have different temperature set-points for the indoor air temperature and domestic hot water, along with different internal heat gains in the building and different heat demand for domestic hot water.

The principle of the aggregation is explained for the case of space heating in figure 4. For each of the 32 buildings with one occupant, the actual lower bound for the indoor air temperature is determined. Thus not the set-point is taken as a lower bound, but the lowest temperature possible if thermal comfort is to be attained. This actual lower bound is determined by taking into account the warm-up and cool-down curve of the building. This bound is thus dependent occupant behaviour, ambient air temperature, building parameters and heating system parameters. The aggregated model then consists of one building model for which the lower temperature bound is the average of the 32 actual lower temperature bounds. The internal heat gains are averaged over the 32 internal heat gain profiles. A similar procedure is followed for domestic hot

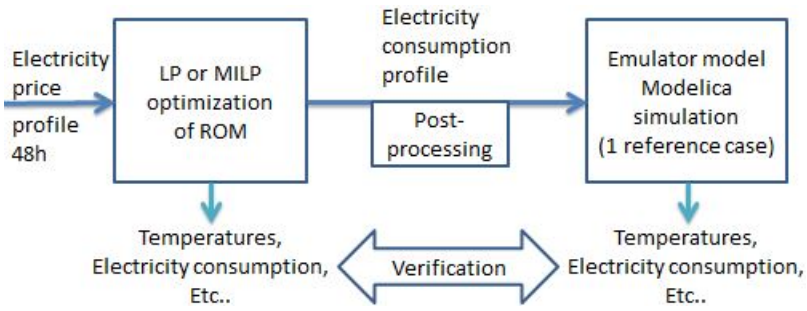

Figure 5: The verification is performed as follows: the outcome of multiple ROMs are compared to a reference emulator model. The reference emulator model tries to track the electricity consumption profile from the ROM as closely as possible.

water: the actual lower bounds for the storage tank temperatures is determined along with the average hot water demand. As there are 6 cases of number of inhabitants, and hence 6 different hot water storage tanks, the aggregated model consists of 6 building models that represent the 100 building models. But these 6 building models could easily represent a thousand or more buildings, since the procedure is the same. The similarity between the two levels of detail is illustrated in section 4.2.

3.4. Summary

The methodology section gives an overview of all modelling levels needed to come up with an aggregated, reduced order model of buildings equipped with heat pumps. The aim of these models is a co-optimization with electricity generation park models in order to investigate the potential for demand side management. Hence, simplifications are needed with respect to the detailed physical model. Whether the simplifications presented in the methodology section can be justified, is discussed in the following section.

4. RESULTS AND DISCUSSION

The results and discussion section is split up into two parts. The first section compares the reduced order model to the emulator model, which is done for multiple user behaviours and multiple hot water storage tank sizes. The second section shows the performance of the aggregation.

4.1. Verification w.r.t. emulator model

The reduced order model is verified with respect to the emulator model as shown in figure 5. For multiple electricity price profiles, the ROM is used in the optimization (Eq. (7)-(10)) determining optimal system operation for a time period of 48 hours. From this optimization, profiles for the electricity consumption, indoor air temperature, COP, etc can be obtained. The verification is done by letting the emulator model track this electricity consumption profile with an intermediate post-processing in some cases. The resulting profiles for indoor air temperature and hot water storage tanks are then compared, as shown in figure 6. In the ROM, the thermal comfort constraints are always met, since these are a constraint in the optimization. Thermal comfort is not always met for the emulator model. As shown in table 2, there are multiple ROM options for all the components. All these model options were compared for three electricity price profiles, namely in the shape of a sine wave with a mean value of $0.10\frac{EUR}{kWh}$ and an amplitude of 0.01, 0.02 and $0.05\frac{EUR}{kWh}$. The results for the three electricity price profiles did not show much

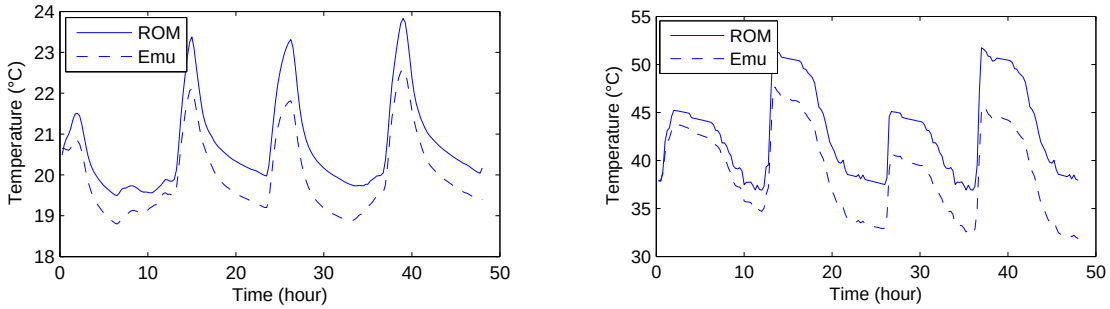

(a) Average indoor operative temperature.

(b) Average DHW tank temperature.

Figure 6: Comparison of some average temperatures over all 25 buildings in case of the ROM and the emulator (Emu) model. The reduced order model approximates the detailed simulation model well, but there is still a (steady-state) deviation between both models.

difference though, therefore the results of this section are only discussed for the electricity price profile with an amplitude of $0.02\frac{EUR}{kWh}$, as shown in Figure 8(a).

Results reference case. As reference case, all model options 2 of table 2 are chosen. So the reference ROM consists of a heat pump with a COP that is a function of the ambient air temperature and has no modulation constraints. The lack of modulation constraints is corrected by performing a post-processing on the electricity demand profile as explained in section 3.2.2. In the reference model, the radiator is also included with a constant UA value and a thermal capacity. Finally, this reference ROM also has the linear, fully mixed model for the domestic hot water tank. Figure 6 shows the indoor operative temperature and DHW tank averaged over the 25 buildings. As can be seen from the figure, these buildings react upon the price profile (Figure 8(a)), preheating the zone and DHW tank when the price is low.

The indoor operative temperature of the ROM shows an almost constant deviation from the emulator model. This is due to two factors, namely a deviation in tracking of the electricity consumption profile and losses in the distribution pipes. Firstly, the emulator model consumes 5% less electricity than the ROM, as shown in figure 8(b). Secondly, the lack of a distribution pipe model in the ROM causes an additional 5% difference in thermal energy supplied. Regarding the thermal comfort in the reference ROM, only the temperatures in periods when thermal comfort is demanded, are important. The distribution of indoor operative temperature when occupants are present is shown in figure 7. The indoor operative temperature drops regularly below the demanded temperature of $20\,°C$ but rarely below $19\,°C$. This deviation is clearly noticeable in figure 6: the indoor operative temperature in the emulator model is between $0.5\,°C$ and $1\,°C$ lower than in the ROM. This causes a substantial thermal discomfort of $3.96Kh$ per building per day with respect to $20\,°C$. When taking a reference temperature of $19.5\,°C$ for the thermal discomfort, this value is $1.04Kh$.

For the DHW tank model, the error of the ROM tends to become larger in time. This is mainly due to a small underestimation of the heat pump's COP, which tends to build up as the simulation time is longer. Figure 7 shows the distribution of temperatures when the occupants tap DHW from the tank. As can be seen from the figure, the temperature at which the DHW is tapped is never below $45\,°C$. The total discomfort for DHW with regard to the reference of $50\,°C$ is $0.87Kh$ per building per day.

Another important aspect of the comparison between ROM and emulator model is how good the emulator model is able to track the electricity consumption profile as determined by the

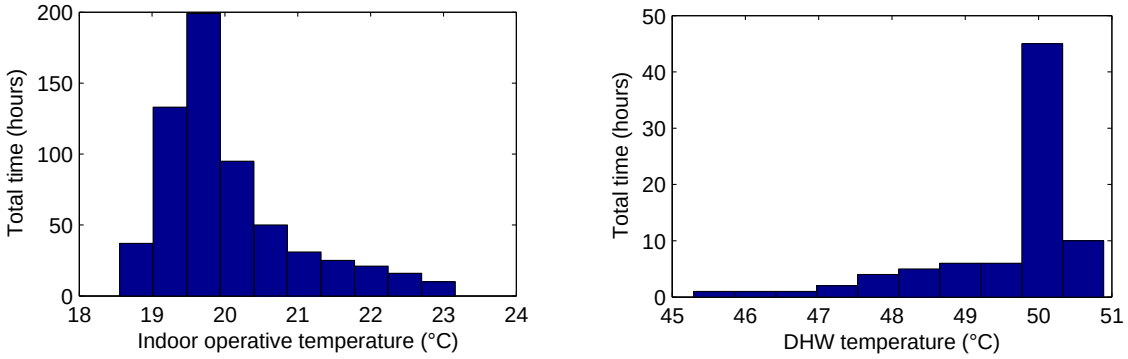

(a) Histogram indoor temperature. (b) Histogram DHW tap temperature.

Figure 7: Histogram of temperature during comfort periods for the 25 buildings. The indoor air temperature that should be above $20\,°C$ *(left). The temperature of the domestic hot water when this is tapped from the tank, should be above* $50\,°C$ *(right).*

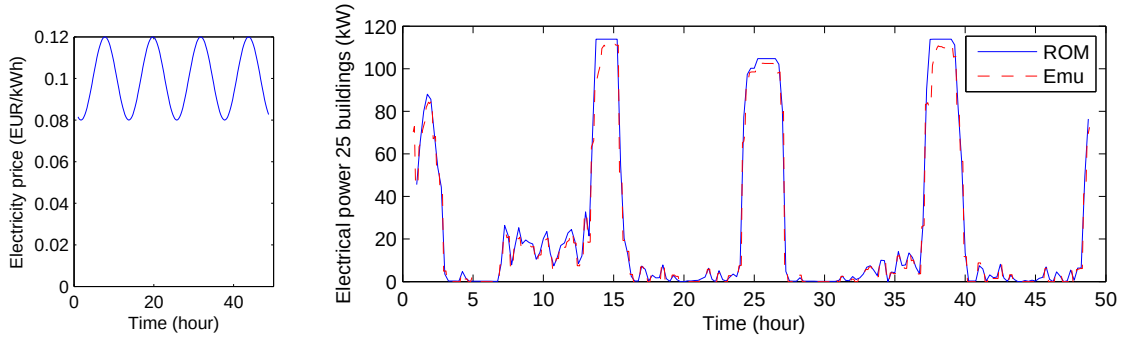

(a) Electricity price. (b) Electricity consumption.

Figure 8: The variation in electricity price (left) induces a reaction of the reduced order model (right). The emulator model (Emu) is not always able to attain the electricity consumption that the reduced order model (ROM) determined.

ROM. This tracking performs well (Figure 8(b)), except when the electricity demand peaks significantly. The emulator model is not able to attain this electric power, especially when starting up. This causes the total electricity consumption of the emulator model to be 4.8% lower than that of the ROM.

Discussion reference case. Table 3 shows the deviation of various ROMs compared to the emulator model. The RMSE on the electric power is about $200W$ per building, which is acceptable given the average power usage of $3500W$ per building when a heat pump is switched on. In the reference case, the deviation of the indoor operative temperature is about $0.8\,°C$. Do note that the deviation of the building linear model with respect to the emulator model is already $0.3\,°C$ (Reynders et al., 2014) (Figure 3). The addition of a ROM for the heating system seems to increase the error on the indoor operative temperature. The DHW tank temperature in the emulator model was usually about $2.7\,°C$ lower than in the ROM, but this did not have a large effect on DWH comfort.

Results and discussion of comparison with other ROM options. Table 3 shows the deviation of various ROM options compared to the emulator model. The cases presented are variations of some aspects of the ROM. There are two other linear models, namely the 'No radiator' case, which leaves out the radiator model, and the 'Constant COP' case, which takes a constant COP

Table 3: Four results of the verification, the first three being the root mean square errors (RMSE) on electric power[W/building]-indoor operative temperature[$^\circ C$]-DHW tank temperature[$^\circ C$] and the last being the calculation time of the ROM optimization [sec]. These quantities are shown for two chosen time steps (15 and 60 minutes).

Time step	15 min	60 min
Reference	208-0.80-2.75-8	375-0.71-3.50-1
No radiator	170-0.90-2.70-5	320-1.05-3.36-1
Constant COP	195-0.73-2.54-6	380-0.60-2.55-1
DHW tank integer	217-0.81-2.62-7200	425-0.70-3.16-7200
Switch SH/DHW	185-0.77-3.01-7200	290-0.70-1.96-7200
Modulation	210-0.71-2.80-7200	(150-0.74-1.35-20)

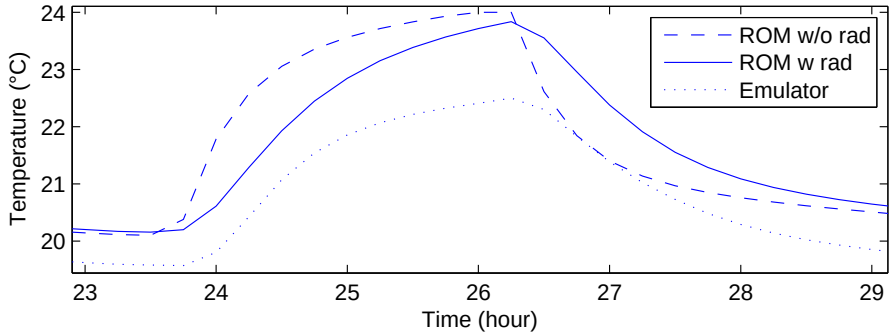

Figure 9: The indoor operative temperature in the case of the reduced order model with (w) and without (w/o) a radiator model included. The ROM without radiator overestimates the rate at which the indoor temperature can rise and drop.

instead of a COP as a function of the ambient air temperature. The other cases include integer variables. In the 'DHW tank integer' case, the higher limit for the DHW tank temperature is given by equations (22)-(23). The 'Switch SH/DHW' case introduces one integer variable to force the heat pump to supply either SH or DHW during a time step. In the final 'Modulation' model, the heat pump model includes boundaries for minimal modulation as given by equations (12)-(15). Table 3 shows that using a smaller time-step lowers the root mean square error (RMSE) on the electric power, but does not always lower the RMSE on the temperatures.

As radiators have a relatively small time constant compared to that of the building structure, one could suggest to neglect it's thermal capacity. Leaving out the radiator lowers the error on the electric power but increases the error on the indoor temperature significantly. As figure 9 shows, this increase is mainly due to different dynamical behaviour, which can be explained by the absence of the thermal capacitance associated to the emission system. Hence the radiator model is not negligible for the dynamic aspects of the model.

Figure 10 shows the COP of the emulator model as compared to that of the ROM with variable COP. Note the large peaks in COP of the former model when the heat pump is switched on. This is because the distribution pipes are still cold at this point in time, allowing a high thermal power at condenser side. A part of this gain in COP is thus directly lost due to intermittent heating of these distribution pipes. As can be seen in Table 3, using a constant COP (3.8 for space heating and 2.4 for DHW) has an overall positive impact on the performance of the ROM, albeit limited in some cases. This is because the constant COP model approximates the COP of the emulator heat pump model 4% better than the reference case. Note that this constant COP

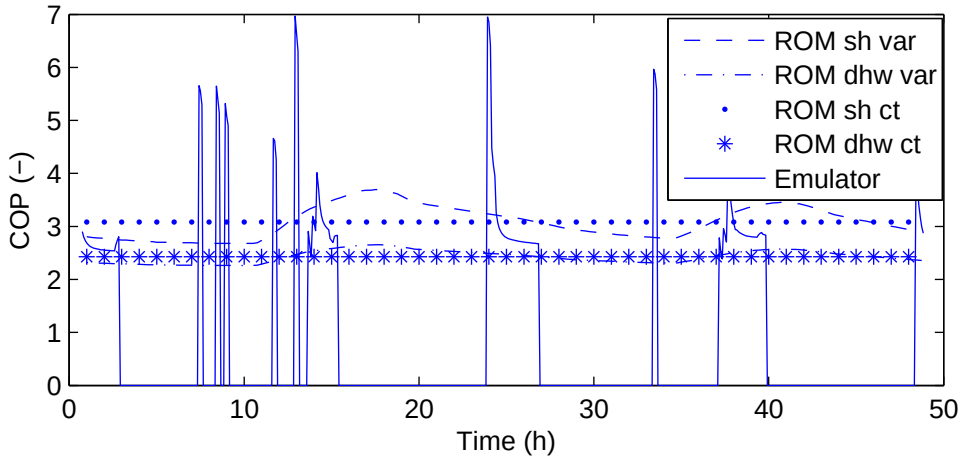

Figure 10: The COP in the reference ROM is either a function of the ambient temperature (var) or constant (ct). As the optimization sometimes chooses to operate the heat pump for only fifteen minutes, the COP in the emulator model can become very high. However, a part of this extra produced heat is lost when the heat distribution system cools down again.

is the average of the COP in the reference case, which changes as a function of the ambient air temperature. The results of the COP are in line with Verhelst et al. (2012), who studied multiple COP formulations, from which there were two linear representations: a constant COP and a COP that is function of the ambient air temperature only. When no electricity price profile was considered, a constant COP formulation performed better, since this formulation did not cause peaks in the electric power of the heat pump. When an optimization towards minimal cost was considered, both COP formulations performed equally.

The cases with integer variables 'DHW tank integer', 'Switch SH/DHW' and 'Modulation' do not show a significant improvement to the performance of the reference model (Table 3). The far longer calculation time (in most cases the maximum calculation time of 7200 seconds) is not worth the minor extra detail these integer variables add. Another possible advantage of the 'Modulation' case, namely the abolishment of a post-processing phase as the electricity usage is conform with the real heat pump constraints, is questionable. The linear reference model (8 seconds) with post processing as discussed in section 3.2.2 (5 seconds) takes up 13 seconds in total, which is a lot faster than the 'Modulation' model.

The results for the case 'Modulation' with a time-step of 60 minutes are put between brackets because it is a special case. When the heat pump would operate at its lower modulation limit (30% of maximal power) for an hour to supply hot water to the DHW tank, the temperature would exceed the upper limit. So the solution attained is one in which the back-up electrical resistance heater covers all DHW demand. As one can note from the table, the model for this alternative heating performs well for the DHW tank temperature.

4.2. Performance of aggregation

As explained in section 3.3, the aim of the aggregation is reducing the number of building ROMs needed. 100 building models with a different number of inhabitants and different user behaviour are aggregated to 6 building models. The way to determine the accuracy of this aggregated model, is to examine whether it attains the same total electricity cost with respect to an identical electricity price profile. Figure 11(a) shows how the total electricity cost per dwelling changes with respect to a higher amplitude of a sine wave electricity price profile around a mean price

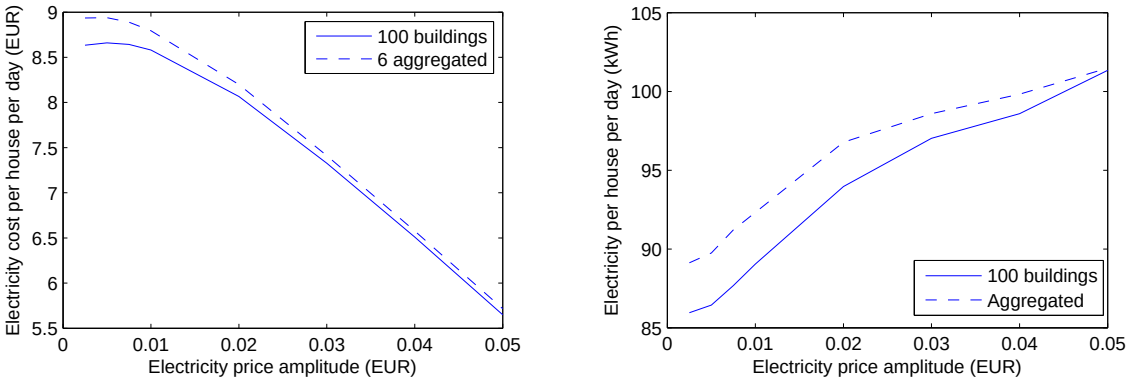

(a) Total electricity cost.

(b) Total electricity consumption.

Figure 11: The total electricity cost per dwelling in case of the original model consisting of 100 buildings and the aggregated model consisting of 6 buildings. In the aggregated case, the total cost is about 1% *to* 3.5% *higher than is possible to attain with the larger cluster of buildings.*

of $0.10\frac{EUR}{kWh}$. As this amplitude increases, the building structure and DHW tank are increasingly used as energy storage, lowering total electricity cost. The aggregated building model shows the same trend, and predicts this cost with an error between 1% and 3.5%. This decrease in total electricity cost has the downside of increasing the energy consumption, as figure 11(b) shows. The electricity consumption of the aggregated model also shows the same trend, being between 0.5% and 4% higher than in the original model.

The comparison between the 100 buildings model and the aggregated 6 buildings model was also performed for random and wholesale market profiles on top of the sine wave electricity price profiles. Figure 12 plots the relative difference in total electricity cost and mean indoor operative and DHW tank temperature between the aggregated and the original model. The aggregated model overestimates the total electricity cost with about 1% to 3.5%, the indoor temperature with -2% to 2% and the DHW tank temperature with 4% to 8%.

A check was also performed, whether the 100 buildings model would be able to track the electricity usage of the aggregated model. This was performed for all price profiles, by minimizing the deviation given the constraints of the 100 buildings model. This check proved to be successful: the deviation on the profile is lower than 0.1%.

Discussion The model with 100 buildings has a slightly higher potential for DSM than the aggregated model: it can lower the electricity cost per building and attain lower energy losses in doing so. This is because the model with 100 buildings has more options to shift some energy demand, as there will always be more opportunities to make a small change in very specific cases. Nevertheless the aggregated model comes very close to the larger model. Since the aggregated model always overestimates electricity cost and consumption, one could say that the aggregated model can act as an lower boundary for the performance of the larger model. In other words, the aggregated model is always a small underestimation of the flexibility potential.

5. CONCLUSION

The aim of this paper is to present a verified, aggregated building stock model, useful for studying the potential of DSM programmes for residences equipped with heat pumps. The mathematical form of the model is chosen such that it can be combined with electricity generation park models (Bruninx et al., 2013). Multiple reduced order models were studied, where the fully lin-

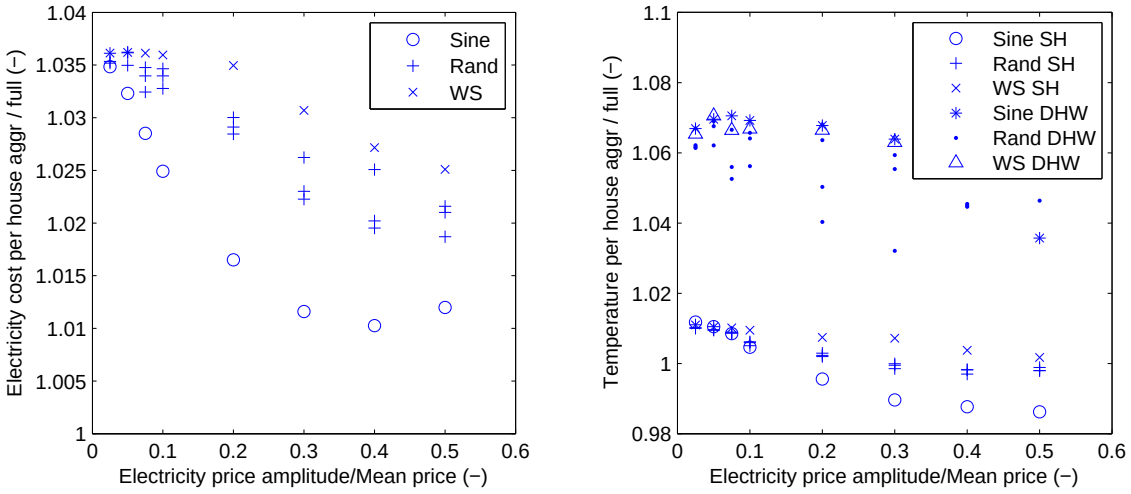

(a) Total electricity cost.

(b) Indoor and DHW temperature.

Figure 12: Difference in total cost, indoor operative temperature (SH) and DHW tank temperature (DHW) in the aggregated case of 6 buildings compared to that of the original model with a 100 buildings. This comparison was done for multiple price profiles with a certain amplitude and a shape based on a sine wave (sine), random (rand) or wholesale market prices (WS).

ear model with radiator model, constant COP and linear formulation of heat pump modulation and DHW tank constraint performed the best. This is because of its favourable computation time and smallest deviation with respect to the detailed physical emulator model: $0.8\,°C$ on the indoor operative temperature and $2.7\,°C$ on the DHW tank temperature. The output of this fully linear model is convertible to control signals to be applied to the physical emulator model or a real-life implementation by a post-processing method discussed in this paper. Additionally, an aggregation method was presented, which is able to reduce the number of buildings needed in order to represent multiple user behaviours. This aggregated model can act as a worst case for the performance of a large cluster of buildings, as it overestimates the costs with 1% to 4%.

6. ACKNOWLEDGEMENTS

The author, Dieter Patteeuw, gratefully acknowledges the KU Leuven for funding his work in the framework of a PhD within the GOA project on a 'Fundamental study of a greenhouse gas emission-free energy system'.

REFERENCES

Baetens, R., De Coninck, R., Van Roy, J., Verbruggen, B., Driesen, J., Helsen, L., & Saelens, D. (2012, August). Assessing electrical bottlenecks at feeder level for residential net zero-energy buildings by integrated system simulation. *Applied Energy*, *96*, 74–83.

Barton, J., Huang, S., Infield, D., Leach, M., Ogunkunle, D., Torriti, J., & Thomson, M. (2013, January). The evolution of electricity demand and the role for demand side participation, in buildings and transport. *Energy Policy*, *52*, 85–102.

Bruninx, K., Patteeuw, D., Delarue, E., Helsen, L., & D'haeseleer, W. (2013). Short-term demand response of flexible electric heating systems: the need for integrated simulations. In *European Energy Market (EEM), 2013 10th international conference on the* (pp. 1–10).

Callaway, D. S. (2009, May). Tapping the energy storage potential in electric loads to deliver load following and regulation, with application to wind energy. *Energy Conversion and Management*, *50*(5), 1389–1400.

Code van goede praktijk voor de toepassing van warmtepompsystemen in de woningbouw [Computer software manual]. (2004).

Cyx, W., Renders, N., Van Holm, M., & Verbeke, S. (2011). *IEE TABULA - typology approach for building stock energy assessment.* (Tech. Rep.). VITO, Belgium (BE).

De Coninck, R., Baetens, R., Saelens, D., Woyte, A., & Helsen, L. (2014, July). Rule-based demand-side management of domestic hot water production with heat pumps in zero energy neighbourhoods. *Journal of Building Performance Simulation*, *7*(4), 271–288.

FOD economy Belgium. (2008). *Structuur van de bevolking volgens huishoudens: per jaar, gewest en aantal kinderen.* Online: $http://statbel.fgov.be/nl/statistieken/cijfers/bevolking/$.

Gellings, C. W. (1985). The concept of demand-side management for electric utilities. *Proceedings of the IEEE*, *73*(10), 1468–1470.

Good, N., Navarro-espinosa, A., Mancarella, P., & Karangelos, E. (2013, May). Participation of electric heat pump resources in electricity markets under uncertainty. In *10th international conference on the European Energy Market (EEM).*

Hedegaard, K., & Balyk, O. (2013, October). Energy system investment model incorporating heat pumps with thermal storage in buildings and buffer tanks. *Energy*, *63*, 356–365.

Hedegaard, K., Mathiesen, B. V., Lund, H., & Heiselberg, P. (2012, November). Wind power integration using individual heat pumps - analysis of different heat storage options. *Energy*, *47*(1), 284–293.

Henze, G. P., Felsmann, C., & Knabe, G. (2004, February). Evaluation of optimal control for active and passive building thermal storage. *International Journal of Thermal Sciences*, *43*(2), 173–183.

Judkoff, R., & Neymark, J. (1995). *International energy agency building energy simulation test (BESTEST) and diagnostic method* (Tech. Rep.). National Renewable Energy Lab., Golden, CO (US).

Kamgarpour, M., Ellen, C., Esmaeil, S., Soudjani, Z., Gerwinn, S., Mathieu, J. L., ... Fr, M. (2013, August). Modeling options for demand side participation of thermostatically controlled loads. In *Symposium-bulk power system dynamics and control -ix (IREP).*

Kelly, N. J., Tuohy, P. G., & Hawkes, A. D. (2013). Performance assessment of tariff-based air source heat pump load shifting in a UK detached dwelling featuring phase change-enhanced buffering. *Applied Thermal Engineering*.

Kersting, W. H. (2012). *Distribution system modeling and analysis*. CRC press.

Koch, T., Achterberg, T., Andersen, E., Bastert, O., Berthold, T., Bixby, R. E., ... Wolter, K. (2011). Miplib 2010. *Mathematical Programming Computation*, *3*(2), 103–163.

Kok, K., Roossien, B., Macdougall, P., van Pruissen, O., Venekamp, G., Kamphuis, R., ... Warmer, C. (2012, July). Dynamic pricing by scalable energy management systems-field experiences and simulation results using powermatcher. In *Power and energy society general meeting.*

Kondoh, J., Lu, N., Member, S., & Hammerstrom, D. J. (2011, July). An evaluation of the water heater load potential for providing regulation service. In *Power and energy society general meeting.*

Kosek, A. M., Costanzo, G. T., Bindner, H. W., & Gehrke, O. (2013). An overview of demand side management control schemes for buildings in smart grids. In *Smart energy grid engineering (SEGE), 2013 IEEE international conference on* (pp. 1–9).

Long, H., Xu, R., & He, J. (2011, October). Incorporating the Variability of Wind Power with Electric Heat Pumps. *Energies*, *4*(10), 1748–1762.

Lu, N., & Vanouni, M. (2013, November). Passive energy storage using distributed electric loads with thermal storage. *Journal of Modern Power Systems and Clean Energy*.

Malhame, R. (1985, September). Electric load model synthesis by diffusion approximation of a high-order hybrid-state stochastic system. *IEEE Transactions on Automatic Control*, *30*(9), 854–860.

Mathieu, J., Dyson, M., & Callaway, D. (2012, August). Using residential electric loads for fast demand response: The potential resource and revenues, the costs, and policy recommendations. In *ACEEE summer study on energy efficiency in buildings.*

Meibom, P., Kiviluoma, J., Barth, R., Brand, H., Weber, C., & Larsen, H. V. (2007, July). Value of electric heat boilers and heat pumps for wind power integration. *Wind Energy*, *10*(4), 321–337. doi: 10.1002/we.22

Meteonorm version 6.1 edition 2009 (Tech. Rep.). (2009). Meteotest.

Muratori, M., Roberts, M. C., Sioshansi, R., Marano, V., & Rizzoni, G. (2013, July). A highly resolved modeling technique to simulate residential power demand. *Applied Energy*, *107*, 465–473.

Patteeuw, D., Bruninx, K., Delarue, E., D'haeseleer, W., & Helsen, L. (2013). *Working paper: Short-term demand response of flexible electric heating systems: an integrated model.*

Pedersen, T. S., Andersen, P., Nielsen, K. M., Stæ rmose, H. L., & Pedersen, P. D. (2011, September). Using heat pump energy storages in the power grid. In *IEEE international conference on control applications (CCA)* (pp. 1106–1111).

Peeters, L., Dear, R. d., Hensen, J., & D'haeseleer, W. (2009). Thermal comfort in residential buildings: comfort values and scales for building energy simulation. *Applied Energy*, *86*(5), 772–780.

Peuser, F., Remmers, K.-H., & Schnauss, M. (2010). *Solar thermal systems, succesful planning and construction*. Berlin, Germany: Beuth Verlag GmbH.

Reynders, G., Diriken, J., & Saelens, D. (2014). Quality of grey-box models and identified parameters as function of the accuracy of input and observation signals. *Energy and Buildings*, *82*, 263–274.

Richardson, I., Thomson, M., & Infield, D. (2008). A high-resolution domestic building occupancy model for energy demand simulations. *Energy and Buildings*, *40*(8), 1560–1566.

Strbac, G. (2008). Demand side management: Benefits and challenges. *Energy Policy*, *36*(12), 4419–4426.

Verhelst, C., Logist, F., Van Impe, J., & Helsen, L. (2012). Study of the optimal control problem formulation for modulating air-to-water heat pumps connected to a residential floor heating system. *Energy and Buildings*, *45*, 43–53.

Wang, D., Parkinson, S., Miao, W., Jia, H., Crawford, C., & Djilali, N. (2012, January). Online voltage security assessment considering comfort-constrained demand response control of distributed heat pump systems. *Applied Energy*, *96*, 104–114.